Molecular Biology of the Cell
Vol. 15, 2073–2083, May 2004

The Tetraspan Protein EMP2 Modulates the Surface Expression of Caveolins and Glycosylphosphatidyl Inositol-linked Proteins

Madhuri Wadehra,* Lee Goodglick,† and Jonathan Braun*†‡

*Molecular Biology Institute and †Department of Pathology and Laboratory Medicine and Jonsson Comprehensive Cancer Center, University of California at Los Angeles, Los Angeles, California 90095

Submitted July 11, 2003; Revised November 14, 2003; Accepted December 9, 2003
Monitoring Editor: Reid Gilmore

Caveolae are a subset of lipid rafts enriched in glycosphingolipids and cholesterol-rich domains, but selectively lacking glycosylphosphatidyl inositol-anchored proteins (GPI-APs). Caveolin proteins are the organizing component of caveolae, but the corresponding proteins for other classes of lipid rafts are poorly defined. Epithelial membrane protein-2 (EMP2), a member of the four-transmembrane superfamily, facilitates plasma membrane delivery of certain integrins. In this study, we found by laser confocal microscopy that EMP2 was associated with GPI-APs (detected by the GPI-AP binding bacterial toxin proaerolysin). Biochemical membrane fractionation and methyl-β-cyclodextrin treatment demonstrated that this association occurred within lipid rafts. EMP2 did not associate with caveolin-bearing membrane structures, and recombinant overexpression of EMP2 in NIH3T3 cells decreased caveolin-1 and caveolin-2 protein levels while increasing the surface expression of GPI-APs. Conversely, a ribozyme construct that specifically cleaves the EMP2 transcript reduced surface GPI-APs and increased caveolin protein expression. These findings suggest that EMP2 facilitates the formation and surface trafficking of lipid rafts bearing GPI-APs, and reduces caveolin expression, resulting in impaired formation of caveolae.

INTRODUCTION

An emerging structural concept for plasma membranes in mammalian cells is the liquid-ordered microdomain. These domains are distinct from the "fluid mosaic" model in that the "liquid-ordered" membranes are more ordered and less fluid than the bulk plasma membrane (Brown and London, 1998b; Brown and London, 2000; Galbiati *et al*., 2001a). Each domain can be defined by its protein and lipid compositions, and it is becoming increasingly clear that these distinct compartments mediate a number of cellular responses from adhesion and signaling to cellular activation (Brown and London, 1998a; Galbiati *et al*., 2001a).

Lipid rafts, defined as the detergent-resistant fraction of the plasma membrane, are 50- to 350-nm domains rich in cholesterol, glycosphingolipids, sphingolipids, saturated phospholipids, and glycosylphosphatidyl inositol-anchored proteins (GPI-APs) (Gruenberg and Maxfield, 1995; Mukherjee *et al*., 1997; Melkonian *et al*., 1999; Abrami *et al*., 2001; Stuermer *et al*., 2001). These dynamic structures also include protein components, reflecting a large (>100) but distinctive set of protein species (Claas *et al*., 2001). Ubiquitously expressed, lipid rafts have been associated with the sorting of proteins bound for the cell surface and the organizing of signaling molecules for efficient transduction (Robinson, 1997; Schmidt *et al*., 2001).

One important subset of lipid rafts are caveolae (Schnitzer *et al*., 1995). Caveolae are 50- to 100-nm membrane invaginations comprised of cholesterol, glycosphingolipids, and at least one member of the caveolin family of proteins. To date, three members of the caveolin family have been identified. Caveolin-1 is the principal component of caveolae in the majority of cell types and is required for their formation (Fra *et al*., 1995; Ostermeyer *et al*., 2001; Razani *et al*., 2001). Caveolin-2 colocalizes with caveolin-1 and shares a similar tissue distribution. Caveolin-3 has a selective tissue distribution and is predominantly expressed in cardiac, smooth, and skeletal muscle cells (Song *et al*., 1996). Caveolae have been implicated in cholesterol trafficking as well as in the regulation of a variety of molecules such as integrins, H-ras, and heterotrimeric G proteins (Wary *et al*., 1998; Sternberg and Schmid, 1999; Moffett *et al*., 2000; Galbiati *et al*., 2001b).

The relationship between caveolae and GPI-AP lipid rafts remains controversial. Reciprocal regulation has been observed between caveolae and GPI-rich raft domains (Abrami *et al*., 2001), and several studies reveal distinctions between GPI-AP lipid rafts and caveolae domains at steady state (Schnitzer *et al*., 1995; Lang *et al*., 1998; Abrami *et al*., 2001; Oh and Schnitzer, 2001; Stuermer *et al*., 2001). Trafficking of GPI-rich rafts largely uses a clathrin-independent endocytic itinerary (Gruenberg and Maxfield, 1995; Mayor *et al*., 1998; Chatterjee *et al*., 2001). On internalization, GPI-APs may be delivered from early endosomes to the Golgi apparatus or back to the plasma membrane via a recycling compartment (Sharma *et al*., 2003). Caveolae are also thought to use a distinct, clathrin-independent intracellular cycling mechanism (Uittenbogaard *et al*., 1998; Uittenbogaard and Smart, 2000). For example, caveolin-1 may move directly from the

Article published online ahead of print. Mol. Biol. Cell 10.1091/mbc.E03–07–0488. Article and publication date are available at www.molbiolcell.org/cgi/doi/10.1091/mbc.E03–07–0488.

‡Corresponding author. E-mail address: jbraun@mednet.ucla.edu.

Abbreviations used: EMP2, epithelial membrane protein-2; GPI, glycosylphosphatidylinositol;GPI-AP,glycosylphosphatidylinositol-anchored protein; GAS3, growth arrest specific-3; PMP22, peripheral myelin protein-22; MβCD, methyl-β-cyclodextrin.

endoplasmic reticulum to the plasma membrane, and the forced overexpression of caveolin-1 can redirect it into lipid storage droplets (Uittenbogaard *et al*., 1998; Ostermeyer *et al*., 2001). However, the mechanisms regulating the trafficking of these proteins are poorly understood.

In this report, we present evidence that epithelial membrane protein (EMP)-2 is involved in determining the formation and/or protein profile of GPI-APs and caveolae lipid raft domains. EMP2 is a member of the growth arrest specific-3/peripheral myelin protein-22 (GAS3/PMP22) family of tetraspan proteins and has recently been found to modulate cellular adhesion properties (Wadehra *et al*., 2002). Other four-transmembrane families, connexins and tetraspanins, have been intensively investigated for their roles in gap junction, cell-cell recognition processes, and intracellular trafficking (reviews in Hemler, 2001; Berditchevski, 2001; Evans and Martin, 2002). Less is known about the GAS3/PMP22 family, pertaining mainly to their association with various disease states. Mutations in the prototypic GAS3 family member PMP22 mediate the neurodegenerative diseases Charcot Marie Tooth (Berger *et al*., 2002) and Dejerrine Sottas Syndrome (Notterpek *et al*., 1999). Disordered expression of EMP3 has been implicated in brain, mammary, and T cell tumors (Ben Porath and Benvenisty, 1996; Ben Porath *et al*., 1999). Similarly, EMP2 has been implicated in B cell tumor progression and stress-induced apoptosis (Wang *et al*., 2001).

Recently, we have observed that EMP2 affects the membrane expression of diverse proteins. EMP2 associates with β1 integrins, reciprocally regulates the repertoire of $\alpha6\beta1$ to $\alpha5\beta1$ on the cell surface, and accordingly regulates the profile of cell-stromal adhesion (Wadehra *et al*., 2002). Because integrin surface display involves lipid rafts, we address in this study whether EMP2 plays a role in lipid raft formation. We show that EMP2 colocalizes with GPI-APs and coexists with them in lipid raft fractions. Elevation of EMP2 expression specifically and dramatically down-regulates caveolin-1 and caveolin-2 expression on the plasma membrane. In contrast, elevated EMP2 expression increased the presence of cell surface GPI-APs raft proteins. Our results thus indicate that EMP2 is an important protein in the formation of caveolae and GPI-AP-lipid rafts.

MATERIALS AND METHODS

Cell Lines

NIH3T3 cells were grown in DMEM (Invitrogen, Carlsbad, CA) plus L-glutamine (2 mM), sodium pyruvate (1 mM), penicillin and streptomycin (100 U/ml) (Invitrogen) with 10% fetal calf serum (Hyclone Laboratories, Logan, UT) at 37°C in a humidified, 5% CO_2 atmosphere (Wadehra *et al*., 2002). We also used NIH3T3 cells stably infected with retroviruses bearing FLAG-tagged murine EMP2 (referred to as 3T3/EMP2 cells), vector control (3T3/V cells), or an EMP2-specific ribozyme (3T3/RIBO cells) (Wadehra *et al*., 2002).

Antibodies

Rabbit polyclonal anti-EMP2 antibodies were reported previously (Wang *et al*., 2001). Anti-adaptin-γ monoclonal antibody (mAb) (clone 88), anti-BIP (clone 40), anti-caveolin-1 (clone 2297), anti-caveolin-2 (clone 65), flotillin 2 (clone 29), and the endosomal proteins rab4 (clone 7) and rab5 (clone 15) were from BD Biosciences (San Diego, CA). A rabbit anti-CDC42 was from Santa Cruz Biotechnology (Santa Cruz, CA). An anti-proaerolysin mAb was obtained from (Protox Biotech, Victoria, BC, Canada)

Confocal Microscopy

NIH3T3, 3T3/V, 3T3/RIBO, or 3T3/EMP2 cells were adhered to glass coverslides overnight at 37°C. To visualize endosomal vesicles, cells were incubated with fluorescein isothiocyanate (FITC)-conjugated transferrin (10 μg/ml; Sigma-Aldrich, St. Louis, MO) for 15 min at 37°C and then fixed with 1.6% formaldehyde. Otherwise, cells were directly fixed with cold methanol (30 min at –20°C) or fixed in 1.6% formaldehyde and permeabilized with phosphate-buffered saline (PBS) + 0.1% Triton X-100 (Pierce Chemical, Rockford, IL) for 10 min at room temperature. Cells were blocked with 1% normal goat serum and incubated with the primary antibody overnight (4°C in a humidified chamber). EMP2 antiserum was used at 1:250 dilution; other primary antibodies were used at 2 μg/ml. Cells were rinsed with PBS + 0.01% Triton X-100 and then incubated (2–4 h. at room temperature) with Texas Red-conjugated donkey anti-rabbit IgG (1:600) or FITC-conjugated donkey antirat IgG (1:50; Jackson ImmunoResearch Laboratories, West Grove, PA). Negative controls included incubation of cells with secondary antibody alone. Cells were copiously washed in PBS + 0.01% Triton, rinsed briefly with double distilled H_2O, and mounted in a 3.5% *n*-propyl gallate-glycerol solution.

Laser scanning confocal microscopy was performed using a Fluoview laser scanning confocal microscope (Olympus America, Melville, NY) with argon and krypton lasers. Light emitted between 525 and 540 nm or above 630 nm was recorded for FITC or Texas Red, respectively. Twenty to 30 horizontal (X,Y) sections were obtained at 0.5-μm intervals. Colocalization experiments were studied in single X-Y optical sections and merged using the Fluoview image analysis software (version 2.1.39). Cells were observed using a 60× oil immersion objective. Experiments were repeated at least three times.

For quantitation of overlap, regions were selected with the most apparent overlap and pixels counted by visual inspection in three to five cells (1000–2000 pixels). As previously described, the total number of pixels of colocalization (yellow) was compared with individual images (green or red) to give a percentage of those pixels containing one marker compared with the other (Nichols *et al*., 2001). Values given represent the mean from three to five separate cells.

Microscopy and Quantitation of Proaerolysin Binding

The toxin proaerolysin and its inactive forms (Protox Biotech) were used to detect all membrane GPI-APs (Diep *et al*., 1998; Barry *et al*., 2001). All proaerolysin variants use membrane GPI as their receptor; the inactive forms fail to form channels and thus do not cause cell death (Diep *et al*., 1998; Barry *et al*., 2001). For confocal microscopy, methanol-fixed cells were immunostained with Alexa 594-conjugated proaerolysin (Protox Biotech) and anti-EMP2 (with FITC anti-rabbit IgG). For flow cytometry, cells were fixed in 2% paraformaldehyde in PBS and incubated with biotin-proaerolysin (gift of Dr. T. Buckley, University of Victoria, Victoria, BC, Canada) for 20 min on ice in PBS + 2% fetal calf serum at 0.4 μg/ml. Cells were washed in PBS and incubated with phycoerythrin-conjugated streptavidin (0.25 μg/million cells) for 30 min on ice (BD Biosciences). Negative control cells were incubated with the secondary antibody alone. After two washes with PBS, cells were analyzed with a FACScan flow cytometer (BD Biosciences). GPI-APs expression levels were calculated as mean fluorescent intensity. Experiments were repeated at least three times.

Aerolysin-mediated Apoptosis

Aerolysin-mediated apoptosis was used as correlate of GPI-APs on the cell surface (Parker *et al*., 1996), because the percentage of killing is proportional to the level of plasma membrane GPI-APs (Parker *et al*., 1996; Nelson *et al*., 1999). A semiconfluent monolayer of cells were incubated for 30 min to 12 h at 37°C in a 5% CO_2 humidified incubator with proaerolysin (0.5 nM) and harvested at indicated times. Cells were resuspended in PBS with 1% calf serum and incubated for 15 min on ice with 0.1 μg propidium iodide and annexin V (BD Biosciences). The percentage of viable cells was quantitated using a FACScan flow cytometer (BD Biosciences). Experiments were repeated three times.

Lipid Raft Fractionation

Cells (5×10^7) were harvested and washed in PBS. Cells were resuspended in Tris-buffered saline (50 mM Tris, pH 7.5, 20 mM EDTA, 10 μg/ml aprotinin, 10 μg/ml leupeptin, 1 mM phenylmethylsuflonyl fluoride, and 1 mM Na_3VO_4) (Moran and Miceli, 1998), and lysed with a Dounce homogenizer (five strokes) or by sonication (Moran and Miceli, 1998; Lusa *et al*., 2001). Samples were then dissolved in 1% Triton X-100 or 1% Brij-58 and incubated on ice for 60 min. The extract was mixed 1:1 with 80% sucrose (40% final), followed by step overlays with 35 and 5% sucrose, and centrifuged at 46,000 rpm for 18 h with a Sorvall SW55 rotor (Global Medical Instrumentation, Albertville, MN). Fractions (400 μl) were collected from the top of the gradient, solubilized in Laemmli buffer, and analyzed by SDS-PAGE.

Cholesterol depletion was performed as described previously (Claas *et al*., 2001). Briefly, cells were washed in PBS to remove serum. Cells were incubated in DMEM containing 20 mM methyl-β cyclodextrin (MβCD; Sigma-Aldrich) for 60 min at 37°C. Cells were analyzed by trypan blue exclusion to insure the lack of toxicity by MβCD before being harvested as described above.

To determine the reversibility of cholesterol depletion with MβCD, cholesterol was replenished exogenously as described previously (Zuhorn *et al*., 2002). After cholesterol depletion, cholesterol (400 μg/ml; Sigma-Aldrich) was added to serum-free media containing 20 mM MβCD for 1.5 h at 37°C. Cells were harvested and used for lipid raft fractionation as described above.

Immunoblot Analysis

Cellular lysates in Laemmli buffer were treated with peptide-N-glycosidase F (New England Biolabs, Beverly, MA) to remove N-linked glycans that interfere with detection of EMP2 epitopes (Wang *et al.*, 2001). Proteins were separated by SDS-PAGE, transferred to a nitrocellulose membrane (Amersham Biosciences, Piscataway, NJ), blocked with 10% low-fat milk in Tris-buffered saline (TBS) and 0.1% Tween 20, and probed with primary antibodies at the manufacturers' recommended dilutions (see figure legends). The membranes were washed in TBS + 0.1% Tween 20, incubated with secondary antibody (Southern Biotechnology Associates, Birmingham, AL; goat anti-rabbit IgG-horseradish peroxidase [HRPO] or goat anti-mouse IgG-HRPO), visualized by chemiluminescence (ECL; Amersham Biosciences), and quantitated using the Personal Densitometer SI and ImageQuanNT software (Molecular Dynamics, Sunnyvale, CA). Negative controls were secondary antibodies alone. Experiments were repeated three times.

Quantitation of EMP2 and Caveolin-1 Levels

To estimate the basal levels of EMP2 and caveolin-1, NIH3T3 and 3T3/EMP2 cells were resuspended at 1×10^4 cells/μl in Laemmli buffer. The cell number equivalents NIH3T3 and 3T3/EMP2 were then titrated down by serial two-fold dilutions of samples and separated by SDS-PAGE. Blots were analyzed for EMP2 and caveolin-1 expression. The experiment was repeated three times independently. Results were averaged, and a SD was calculated.

Northern Blot Analysis

Total RNA was prepared using a RNA purification kit from 3T3/V, 3T3/EMP2, and 3T3/RIBO cells (QIAGEN, Valencia, CA). Total RNA (5 μg) was separated on a 1% formaldehyde/agarose gel and transferred to a nylon membrane. Caveolin-1 and -2 cDNA fragments were generated as described previously (Gargalovic and Dory, 2001). The caveolin-1 fragment generated recognizes both predicted splice variants (Kogo and Fujimoto, 2000). Purified cDNA was used to generate a ^{32}P-labeled probe using random primer synthesis (Amersham Biosciences). Membranes were prehybridized with RapidHyb buffer (Amersham Biosciences) for 1 h and then hybridized with labeled probe overnight at 65°C. Blots were washed with a high stringency buffer (60°C, 0.1× SSC, and 0.5% SDS) and exposed to x-ray film.

Proaerolysin Overlay Assays

To visualize GPI-APs, a proaerolysin overlay assay was performed as described previously (Diep *et al.*, 1998; Sotgia *et al.*, 2002). Briefly, lysates were separated and transferred as described above. Cells were then blocked and incubated at room temperature for 1 h with 20 nM proaerolysin (Protox Biotech) in TBS + 0.1% Tween. Membranes were washed three times and then incubated with a 1:4000 anti-aerolysin mAb probe. After washing three times, membranes were incubated with an anti-mouse IgG-HRPO. Bound immunoglobulin was detected using chemiluminescence (ECL-Plus; Amersham Biosciences)

Cholesterol Determination

Cholesterol levels were assayed using the Cholesterol 20 kit (Sigma-Aldrich). This assay uses cholesterol oxidase to produce hydrogen peroxide. This is then detected in a coupled colorimetric peroxidase assay at absorbance 490 nm. Absorbances were analyzed against cholesterol standards (Sigma-Aldrich) to determine concentrations in micrograms per deciliter.

GPI-APs Dot Blot

To determine GPI-APs expression via sucrose gradient centrifugation, 1 μl of each fraction was blotted onto a nitrocellulose membrane (Amersham Biosciences). After drying, the membrane was blocked in 1% milk for 1 h at room temperature. GPI-APs expression was determined using biotin conjugated-proaerolysin, washing in TBS + 0.1% Tween 20, and detection with HRPO-linked streptavidin (Dako, Carpinteria, CA). The membrane was extensively washed with TBS + 0.1% Tween 20 and analyzed by chemiluminescence.

RESULTS

EMP2, Caveolin-1, and GPI-APs Exist in Detergent-resistant Membrane Fractions

Lipid rafts exist in a separate biophysical phase from the rest of the membrane bilayer (Brown and London, 1997; Schroeder *et al.*, 1998; Brown and London, 1998a,b). These detergent-resistant membranes are rich in cholesterol and sphingolipids, and lipid raft-associated molecules can be isolated using cold nonionic detergents (Claas *et al.*, 2001). Both GPI-APs and caveolin-1 have been localized within lipid rafts (Mayor *et al.*, 1998; Lipardi *et al.*, 2000; Sotgia *et al.*, 2002; Schubert *et al.*, 2002). Because many integrins associate with raft structures and EMP2 colocalizes with integrins (Claas *et al.*, 2001; Leitinger and Hogg, 2002), we postulated that EMP2 may also reside within a lipid raft structure.

Associations within lipid raft gradients can be sorted by hydrophobic detergents (Claas *et al.*, 2001). Robust associations within rafts can be discerned using Triton X-100, whereas specific yet less stringent associations are revealed with 1% Brij-58. To biochemically resolve the lipid raft segregation of EMP2, GPI-APs, and caveolin-1 within NIH3T3 and 3T3/EMP2 cells, lysates were centrifuged using discontinuous sucrose density gradients in the presence of 1% Brij-58 (Figure 1, A and B) or 1% Triton X-100 (Figure 1C). Using 1% Brij-58, EMP2 and GPI-APs were present in the light detergent-resistant membrane fractions 2–5 in both NIH3T3 and 3T3/EMP2 cells (Figure 1, A and B). As expected, in NIH3T3 cells, caveolin-1 also resided in these fractions (Figure 1A). Peak fractions for EMP2 and caveolin-1 differed, suggesting heterogeneity in lipid raft species bearing these proteins. More significantly, no caveolin-1 expression was detectable in any fraction in 3T3/EMP2 cells (our unpublished data; see below).

To confirm the localization of EMP2 to lipid rafts, lysates were prepared in 1% Triton X-100 in the presence or absence of MβCD. β-Cyclodextrins are heptasaccharides that selectively deplete cholesterol from cellular membranes (Claas *et al.*, 2001). Partial depletion of cholesterol typically leads to loss of protein localization into rafts, including GPI-APs (Mayor *et al.*, 1998; Harder *et al.*, 1998). In 1% Triton X-100, EMP2 localized to both light, detergent-resistant fractions 3 and 4 as well as dense fractions 6–9 (Figure 1C). As expected, in 1% Triton X-100, CD9 was only present in dense fractions 8–11. When cells were then incubated for 60 min with MβCD in serum-free conditions, EMP2 expression completely shifted to soluble, dense fractions in the presence of 1% Triton X-100 (fractions 6–11). These data suggest a specific association of EMP2 within lipid rafts. To determine the reversibility of MβCD treatment, cholesterol was added to cells in serum-free media containing MβCD. Cholesterol repletion was sufficient to shift EMP2 into light fractions 3 and 4.

EMP2 Does Not Localize with Caveolin-1

We next examined whether EMP2 was present in surface caveolae or vesicles. Members of the caveolin protein family (caveolin-1, -2, and -3) are critical for caveolae formation, organization, and/or function, and caveolae-like vesicles use a nonconventional trafficking itinerary (Uittenbogaard *et al.*, 1998; Uittenbogaard and Smart, 2000; Sotgia *et al.*, 2002). To determine whether EMP2 localized with caveolin-1 and caveolae membrane domains, the relative distribution of EMP2 to caveolin-1 in NIH3T3 cells was determined by confocal microscopy. As shown in Figure 2, double immunostaining showed no colocalization between EMP2 and caveolin-1 in vesicles or on the plasma membrane surface, suggesting that EMP2 was not associated with caveolae.

We considered that the intracellular vesicles bearing EMP2 might be related to a clathrin-dependent endocytic compartment. This was assessed using FITC-transferrin bound to its receptor after internalization (Nichols *et al.*, 2001). As shown in Figure 3, A–D, only $\leq$20% of the internalized transferrin-bearing vesicles colocalized with EMP2. In addition, we examined colocalization of EMP2 with rab4 and rab5. Rab4 and rab5 are small GTP binding molecules localized primarily to early and recycling endosomes (Daro *et al.*, 1996; Roberts *et al.*, 2001; Sabharanjak *et al.*, 2002). Using monoclonal antibodies for rab4 (Figure 3, E–H) and rab5 (our unpublished data), a similar pattern was observed.

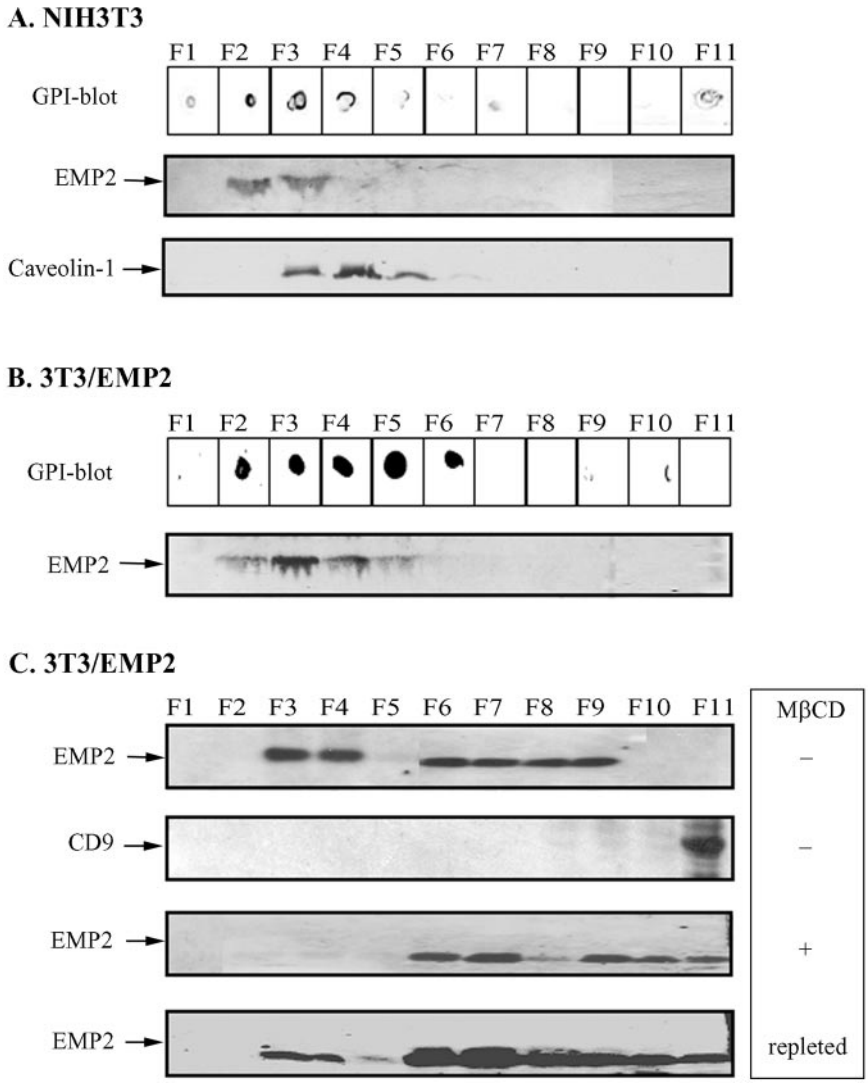

Figure 1. EMP2 is targeted to lipid rafts and is disrupted after MβCD treatment. (A and B) Lipid raft fractionation by Brij-58 insolubility. Cells were lysed in 1% Brij-58 and centrifuged in a sucrose density gradient. Eleven fractions (400 μl each) were collected from the top of the gradient and tested for GPI-APs by proaerolysin dot blot, and for EMP2 (~M_r 20 kDa) and caveolin-1 (~M_r 22 kDa) by using SDS-PAGE and Western blot analysis. (A) NIH3T3. (B) 3T3/EMP2. (C) Cholesterol dependence of EMP2 lipid raft fractionation. 3T3/EMP2 cells were preincubated in the presence (+) or absence (−) of MβCB and then lysed in 1% Triton X-100, gradient fractionated, and EMP2 detected by Western blot analysis. To confirm the reversibility of MβCD treatment, cholesterol was repleted in MβCB-treated 3T3/EMP2 cells and subsequently analyzed by gradient fractionation. The distribution of CD9 (~M_r 24 kDa) in the fractionation was used as a control. Experiments were performed independently three times with similar results.

Less than 10% of rab 4 vesicles associated with EMP2. These findings suggest that intracellular EMP2 largely localizes to vesicles not associated with clathrin-, rab-4–, and rab-5–dependent endosomes.

EMP2 Down-Regulates Caveolin-1 and Caveolin-2

We were intrigued by the apparent loss of caveolin-1 expression in lipid raft fractions from 3T3/EMP2 cells. To better understand the effect of EMP2 on caveolin-1 localization and expression, we evaluated NIH3T3 transfectants with either increased expression (3T3/EMP2 cells) or decreased expression (3T3/RIBO cells; Figure 4A). Using Western blot analysis, cell extracts were analyzed from 3T3/V, 3T3/EMP2, and 3T3/RIBO cells and probed with antibodies against caveolin-1 or caveolin-2 (Figure 4A). Overexpression of EMP2 abolished detectable caveolin-1 protein expression, and caveolin-2 protein was reduced by 10-fold compared with wild-type cells. Conversely, the ribozyme knockout of EMP2 increased the levels of caveolin-1 and caveolin-2 approximately three- and twofold, respectively, compared with wild-type cells (Figure 4A). Neither elevated nor suppressed EMP2 expression affected the protein levels of other endosome-associated proteins (rab4, rab5, CDC42, or flotillin-2).

To quantitate the ratio of caveolin-1 to EMP2 expression, titrations of cell lysates to determine cell number equivalents giving the same signal by Western blot analysis was performed (our unpublished data). For caveolin-1, 3T3/EMP2 cells were reduced 13-fold (±2) compared with wild-type cells. For EMP2, 3T3/EMP2 cells were increased fivefold compared with wild-type cells. This indicated that the changes in EMP2 and caveolin-1 were greater than a 1:1 stoichiometry.

Caveolae require cholesterol for the proper structure and function (Fielding and Fielding, 1996; Uittenbogaard and Smart, 2000). We therefore wondered whether the large reduction in caveolin proteins might be due to an effect of EMP2 overexpression of cellular cholesterol levels. However, 3T3/EMP2, 3T3/V, and 3T3/RIBO displayed no significant difference in total cellular cholesterol: 8.3 ± 0.02 μg/dl, respectively.

EMP2 Alters Caveolin-1 Steady-State mRNA Levels

We next considered the possibility that reduced caveolin proteins with EMP2 overexpression was related to a reduction in steady-state mRNA levels. Total RNA was prepared from 3T3/V, 3T3/EMP2, and 3T3/RIBO cells, and probed for caveolin-1 and -2 (Figure 4B). EMP2 overexpression was

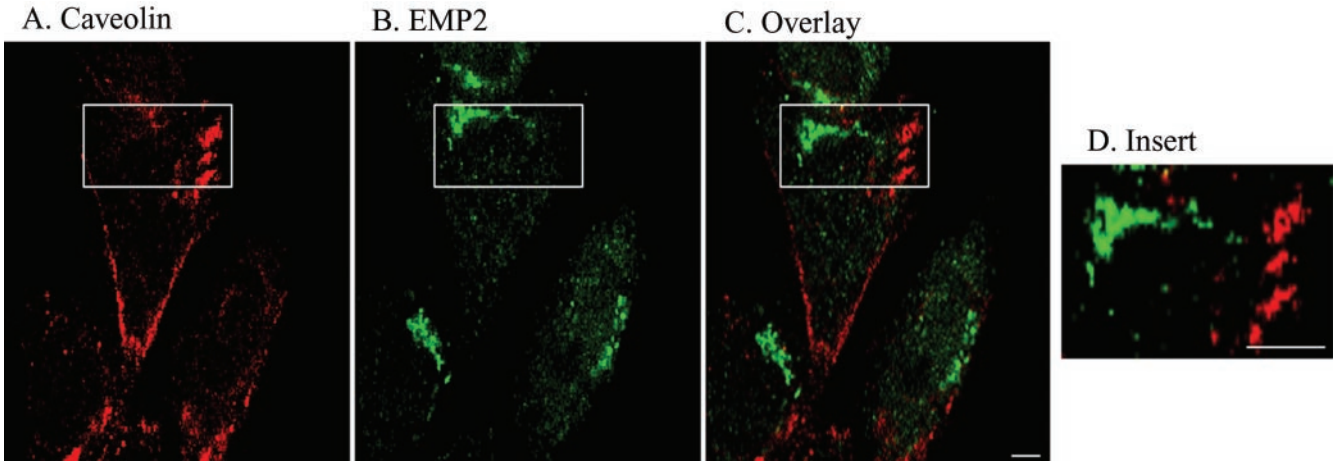

Figure 2. Relationship of EMP2 to caveolin-1. NIH3T3 cells were fixed in cold methanol, immunostained with anti-caveolin-1 (Texas-Red, A) and anti-EMP2 (FITC, B), and compared in single plane overlay images (C). Enlargement of single plane overlap is shown in D. Three independent experiments yielded similar results. Magnification, 600×. Bar, 10 μM.

associated with a moderate threefold reduction in caveolin-1 mRNA. Conversely, 3T3/RIBO cells displayed a modest increase (50%) in caveolin-1 mRNA levels. Caveolin-1 has two isoforms that are generated by alternative transcription initiation (Kogo and Fujimoto, 2000). Interestingly, both mRNA variants can be detected in 3T3/RIBO cells. EMP2 expression did not have an effect on caveolin-2 mRNA levels (Figure 4B).

EMP2 Increases the Levels of Cell Surface GPI-linked Proteins

The relationship between GPI-APs and caveolin-1 remains controversial. Some studies have suggested a reciprocal regulation between caveolae and GPI-anchored protein levels (Abrami *et al*., 2001; Stuermer *et al*., 2001; Sabharanjak *et al*., 2002), whereas others suggest a direct relationship (Sotgia *et al*., 2002; Nichols, 2002). We assessed the effect of EMP2 on the relative GPI-AP surface expression by using 3T3/EMP2, 3T3/V, and 3T3/RIBO cells. Cells were incubated with biotin-conjugated proaerolysin and analyzed by flow cytometry. Compared with vector control cells, we found that 3T3/EMP2 cells displayed an approximately twofold increase in GPI-APs on the plasma membrane (Figure 5A).

The active toxin aerolysin can induce cell death in live cells by binding to GPI-APs (Diep *et al*., 1998; Nelson *et al*., 1999). Therefore, it can be used as a functional assay to

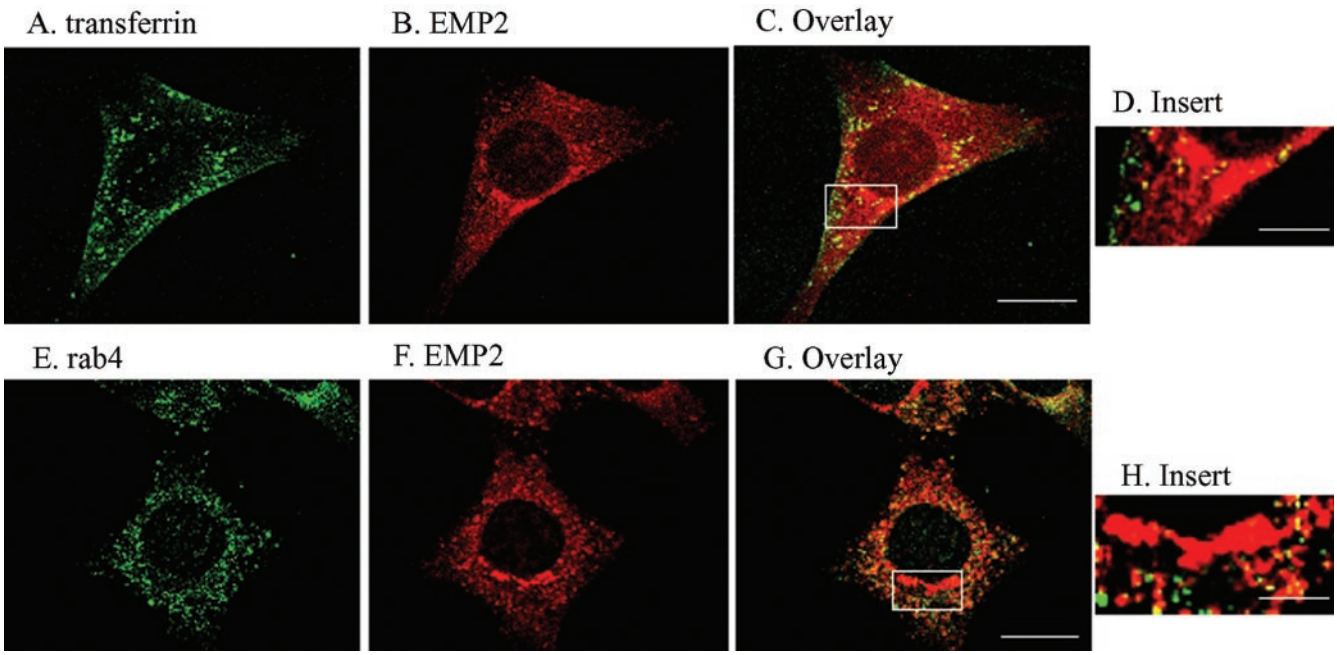

Figure 3. Relationship of EMP2 to endocytic machinery. (A–D) Transferrin. Cells were incubated for 10 min with FITC-conjugated transferrin, fixed in 1.6% formaldehyde, permeabilized with 0.1% Triton X-100, and stained for EMP2 (Texas-Red). Transferrin (A), EMP2 (B), and single plane overlay (C). (E–H) Rab4. Cells were fixed in cold methanol, immunostained with anti-rab4 (FITC, E) and anti-EMP2 (Texas-Red, F), and compared in single plane overlay (G). D and H show enlargements of single plane overlaps. Magnification, 600×. Bar, 15 μM for all panels except D and H (5 μM). Experiments were performed independently three times with similar results.

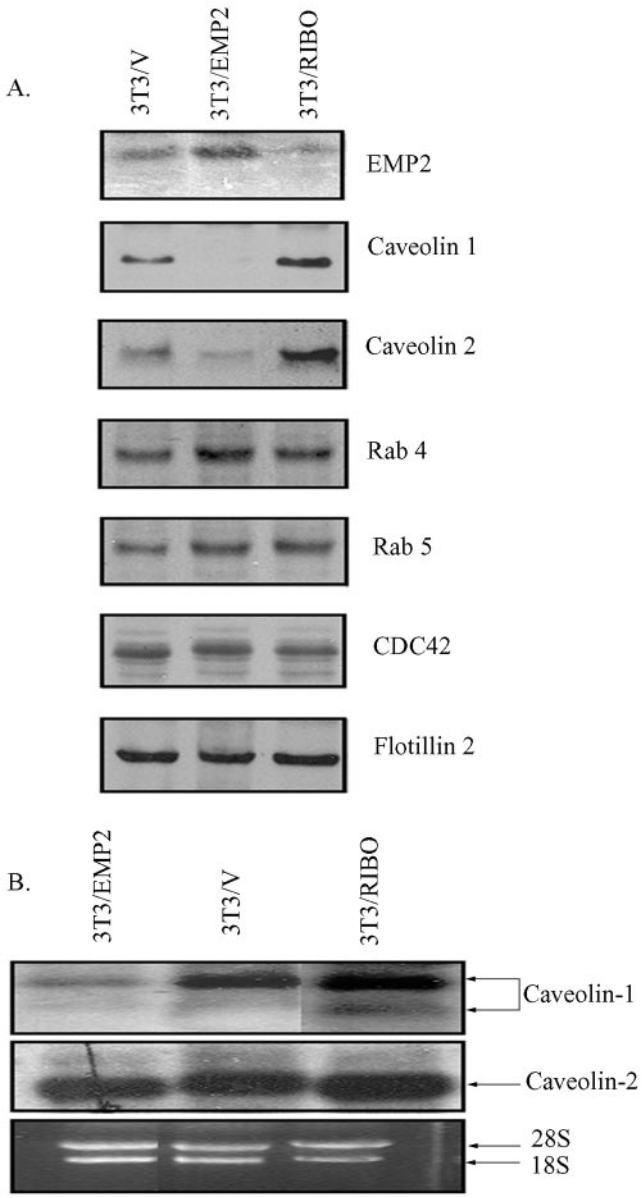

Figure 4. EMP2 expression reduces caveolin-1 and caveolin-2 levels. (A) Steady-state protein levels of caveolin-1 and caveolin-2 were measured by Western blot analysis in cells with varying levels of EMP2 protein. Compared with control cells (3T3/V), caveolin-1 and caveolin-2 were reduced in 3T3/EMP2 cells (high EMP2) and elevated in 3T3/RIBO cells (minimal EMP2). EMP2 expression levels had no influence on proteins associated with the endosomal vesicles (rab4, rab5, and cdc42) or raft structures (flotillin-2). Experiments were performed independently at least three times with similar results. (B) Steady-state caveolin-1 (2.7-kb and 2.1-kb) and caveolin-2 (2.5-kb) mRNA levels were measured by Northern blot analysis in cells with varying EMP2 levels. EMP2 expression reduced caveolin-1 levels but did not affect caveolin-2. The 28S and 18S rRNA species were visualized by ethidium bromide staining and served as a control for equal loading.

assess the levels of plasma membrane GPI-APs. Cells were incubated with 0.5 nM proaerolysin, and assessed after 0, 0.5, 2, and 12 h for viability (propidium iodide) and apoptotic changes (annexin V). Cell death increased with time (our unpublished data), and the 0.5-h group is illustrated (Figure 5, B–D). As predicted, cells with suppressed or endogenously low EMP2 (3T3/RIBO and 3T3/V) had modest or minimal cell death (16 and 9%, respectively; Figure 5, B and C). In fact, the only dead cells in the 3T3/RIBO population were those failing to express GFP/RIBO (Figure 5B). In contrast, extensive cell death (67%) was observed in 3T3/EMP2 cells (Figure 5D) compared with the untreated control (4%; Figure 5E). These results confirm the relationship between increased EMP2 levels and increased GPI-APs on the plasma membrane.

To elucidate the effect of EMP2 on GPI-APs, Western blot analysis was performed on total cell lysates (Figure 5F). In lysates from 3T3/EMP2 cells, there seems to be a marginal increase in a GPI-AP at $\sim M_r$ 26 kDa, whereas both 3T3/V and 3T3/RIBO display similar levels of GPI-APs.

EMP2 Localizes with GPI-APs

GPI-anchoring is important for the membrane trafficking of several proteins such as folate receptor and CD59 (Nichols *et al*., 2001). GPI-APs are lipid raft-associated proteins that seem to be internalized largely via a nonclathrin-mediated route and use endosomes often devoid of markers associated with the clathrin-mediated pathway (Schnitzer *et al*., 1995; Mayor *et al*., 1998; Nichols *et al*., 2001; Chatterjee *et al*., 2001; Nichols, 2000; Sabharanjak *et al*., 2002). To determine whether EMP2 localized to vesicles containing GPI-APs, double immunostaining was performed in wild-type or EMP2-overexpressing cells (Figure 6). We used the bacterial toxin aerolysin, which selectively recognizes the core glycan-peptide of the GPI anchor, to measure all GPI-APs (Parker *et al*., 1996; Diep *et al*., 1998; Nelson *et al*., 1999; Fivaz *et al*., 2001). In wild-type NIH3T3 cells, EMP2 and GPI-APs were mainly confined to cytoplasmic compartments, and partial colocalization was observed in a perinuclear region typical of endoplasmic reticulum (ER)/Golgi staining (Figure 6, C and D). A similar staining pattern was observed for GPI-APs in 3T3/RIBO cells (our unpublished data). However, in 3T3/EMP2, EMP2 and GPI-APs were also present on the plasma membrane and were colocalized in this compartment (Figure 6, G and H).

EMP2 Is Abundant in the Golgi Apparatus

NIH3T3 and 3T3/EMP2 cells express substantial levels of perinuclear intracellular EMP2 (Wadehra *et al*., 2002) and GPI-APs, and it is known that many GPI-APs accumulate within the Golgi apparatus (Nichols *et al*., 2001). To determine the localization of EMP2 within these cells, confocal microscopy was performed with monoclonal antibodies to the adaptor protein-1 complex (AP-1) protein γ-adaptin (Figure 7, A–C and G–I) and the ER chaperone protein BIP (Figure 7, D–F and J–L). EMP2 partially resided within the Golgi apparatus as visualized by its colocalization with γ-adaptin (Figure 7, C and I). Although EMP2 colocalized with γ-adaptin in the Golgi apparatus, it did not seem to be a member of the AP-1 complex, because there was incomplete cytoplasmic colocalization between these two proteins (Figure 7C). In contrast, minimal colocalization was observed between EMP2 and BIP in NIH3T3 cells (Figure 7F). However, there was partial colocalization with BIP in 3T3/EMP2 cells, suggesting that ectopic overexpression of EMP2 causes some accumulation within the ER. It thus seems that the perinuclear localization of EMP2 mainly reflects a prominent Golgi pool.

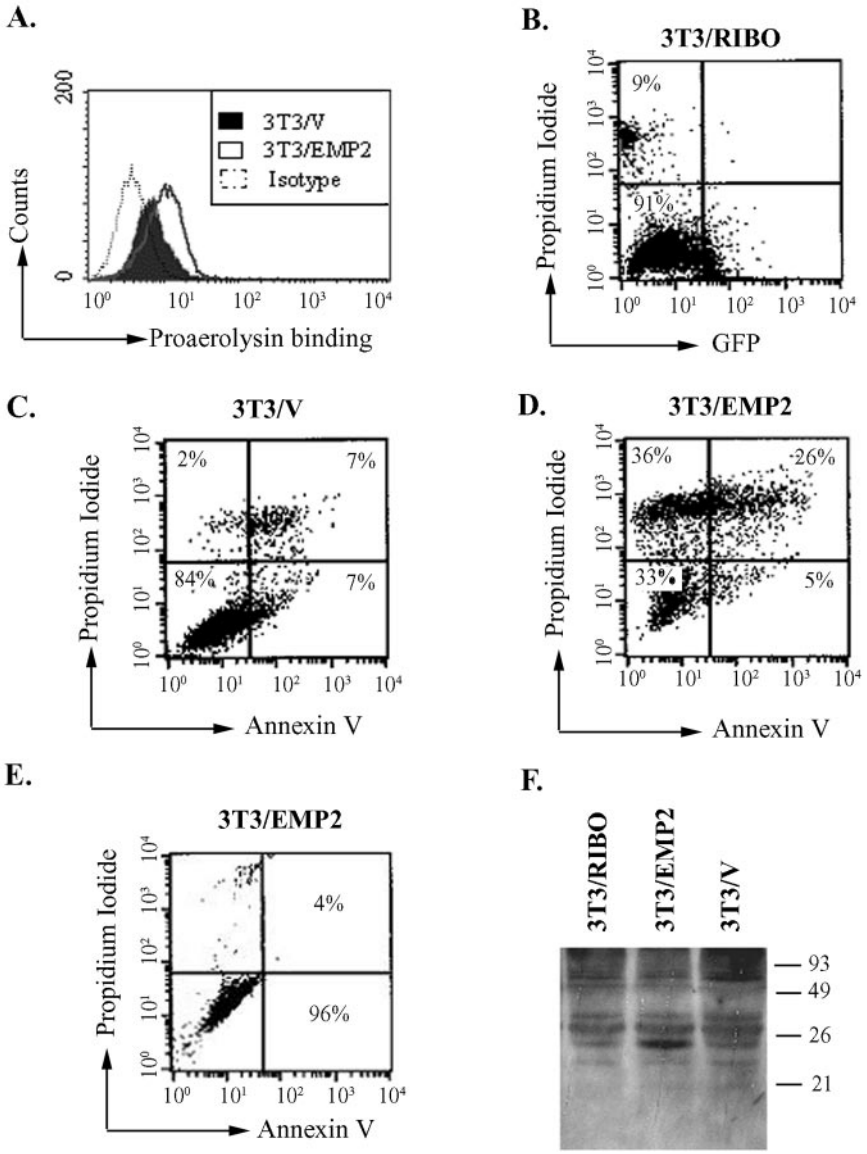

Figure 5. 3T3/EMP2 cells express increased levels of GPI-anchored surface membrane proteins. (A) 3T3/EMP2 and 3T3/V were stained for GPI-APs by using biotin-proaerolysin/phycoerythrin-streptavidin and quantitated by flow cytometry. 3T3/EMP2 cells were approximately twofold increased for surface GPI-APs compared with vector control cells. (B–D) Quantitation of aerolysin-induced cell death. Cells were incubated with 0.5 nM aerolysin for 30 min, harvested, and stained with propidium iodide and annexin V. (B) Propidium iodide and green fluorescent protein (GFP) in 3T3/RIBO cells. Cell death was minimal in cells expressing the GFP-ribozyme transgene but predominant in the GFP-negative nonexpressing subpopulation. (C and D) Propidium iodide and annexin V in 3T3/V (C) and 3T3/EMP2 (D). Cell death was low in vector control cells (16%), and high in EMP2-overexpressing cells (67%). (E) Propidium iodide and annexin V in untreated 3T3/EMP2. Minimal cell death was observed in control cells (4%). Experiments were performed independently at least three times with similar results. (F) 3T3/EMP2, 3T3/V, and 3T3/RIBO cell lysates were analyzed by an aerolysin overlay assay for GPI-APs. 3T3/EMP2 cells display a modest increase in a GPI-AP at ~M_r 26 kDa, whereas 3T3/V and 3T3/RIBO display similar levels of GPI-APs.

DISCUSSION

Caveolae and GPI-rich lipid raft domains exist within the plasma membrane of most mammalian cells. An emerging but as yet unsettled idea is that these represent microanatomically and functionally distinct domains related by reciprocal negative regulation (Abrami *et al*., 2001; Sabharanjak *et al*., 2002). Our present findings add new evidence for this cross talk and indicate that the tetraspan protein EMP2 can affect it through the reciprocal regulation of caveolae and GPI-rich raft domains.

EMP2 in wild-type NIH3T3 cells is predominantly intracellular, but recombinant EMP2 overexpression results in prominent plasma membrane localization. The endosomal pathway of EMP2 was distinct from the vesicular trafficking of the caveolins. Caveolins are thought to use an unusual endocytic itinerary and reside in lipid droplets (Ostermeyer *et al*., 2001; Galbiati *et al*., 2001a). EMP2 was not associated with caveolin-1 trafficking, as demonstrated by its lack of colocalization by confocal immunofluorescence. However, ectopic up- or down-expression of EMP2 reciprocally regulated the protein levels of both caveolin-1 and -2. The influence of EMP2 on caveolin was specific, because EMP2 levels did not alter the levels of clathrin (CDC42 and rab4/5) or lipid raft (flotillin-2) trafficking proteins.

Although EMP2 levels did not substantially alter GPI-APs levels (Western blot), EMP2 did concordantly regulate their surface expression (proaerolysin binding). In NIH3T3 cells, EMP2 colocalized with GPI-APs within lipid raft domains. Like EMP2, GPI-APs is largely clathrin and rab5 independent (Mayor *et al*., 1998; Mayor, 1999; Nichols *et al*., 2001; Chatterjee *et al*., 2001; Sabharanjak *et al*., 2002; Nichols, 2002; Sharma *et al*., 2003). Together, we speculate that GPI-APs-bearing vesicles contain EMP2 and that this association facilitates their plasma membrane trafficking.

Do other tetraspan proteins also act in this manner? A recent study by Hasse *et al.* (2002) proposes that another GAS3 family member, PMP22, resides within detergent-resistant membranes fractions in neuronal cells (Hasse *et al*., 2002). Compared with most tetraspan proteins, EMP2 and PMP22 are particularly similar with respect to amino acid identity (~40%) (Taylor and Suter, 1996), functional phenotype (e.g., susceptibility to apoptosis) (Brancolini *et al*., 2000;

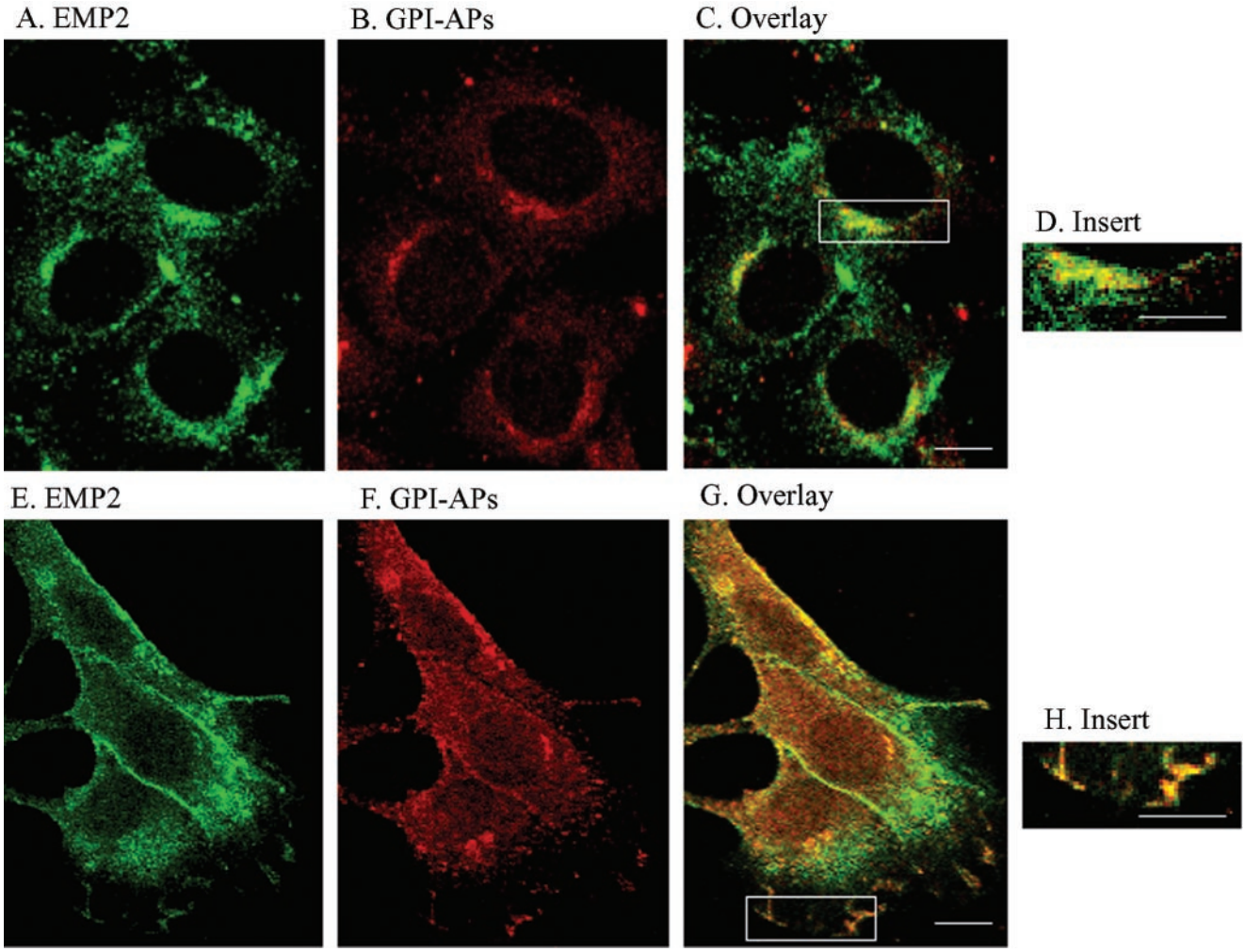

Figure 6. Colocalization of EMP2 and GPI-APs. NIH3T3 cells (A–D) or 3T3/EMP2 (E–H) were fixed in cold methanol, immunostained with proaerolysin (Alexa-594; A and E) and anti-EMP2 (FITC; B and F), and viewed alone or in single plane overlap (C and G). Enlargements of single plane overlaps are viewed in D and H. Experiments were performed independently three times with similar results. Magnification, 600×. Bar, 10 μM.

Wang *et al*., 2001; Sancho *et al*., 2001), and intracellular localization (Tobler *et al*., 1999; Wang *et al*., 2001). Thus, we speculate that EMP2 and PMP22 (and potentially other members of this tetraspan subfamily) have overlapping and/or similar functions.

Studies of the tetraspanin family (e.g., CD9 and CD81) also document their association with lipid raft microdomains and certain integrin isoforms (Berditchevski and Odintsova, 1999; Claas *et al*., 2001). This has prompted the idea that tetraspanins serve as adaptors in the assembly of protein complexes within the plasma membrane (Maecker *et al*., 1997), consistent with the trafficking role proposed here (Berditchevski and Odintsova, 1999). Despite these similarities, EMP2 and tetraspanins function differently. Tetraspanins with the exception of CD81 have little impact on cellular adhesion (Levy *et al*., 1998; Berditchevski and Odintsova, 1999). Moreover, with one exception (CD63) they are not associated with the trafficking of proteins (Kobayashi *et al*., 2000). Also, they reside in distinct endosomal compartments (typically, major histocompatibility complex class II compartments) (Rubinstein *et al*., 1996) and are associated with distinct integrin isoforms. EMP2 does not colocalize with CD9 and thus does not seem to associate with the major histocompatibility complex class II compartment endosomal pathway (Wadehra *et al*., 2002). Thus, if tetraspanins play a role in lipid rafts, their membrane protein and trafficking specificity are nonredundant with EMP2.

The intracellular compartment includes vesicles associated with clathrin-related endosomes and may thus participate in this pathway of sorting endosomes, the pericentriolar recycling endosomal compartment, and late endosomes (Gruenberg and Maxfield, 1995; Mukherjee *et al*., 1997). The intracellular trafficking route of EMP2 seems largely distinct from conventional endosomal compartments. The nontrivial colocalization of EMP2 with these elements might indicate some EMP2 communication with the clathrin-dependent endocytic pathway. In support of this idea, a pool of GPI-APs has been shown to colocalize with transferrin in early endosomes upon internalization from the plasma membrane, and it is possible that the colocalization of EMP2 with transferrin may be specific for early endosomes (Sharma *et al*., 2003). However, the majority of EMP2 did not colocalize with transferrin, rab4, or rab5, and hence did not seem to use the conventional clathrin-dependent, rab protein-regulated receptor pathway. Moreover, the colocal-

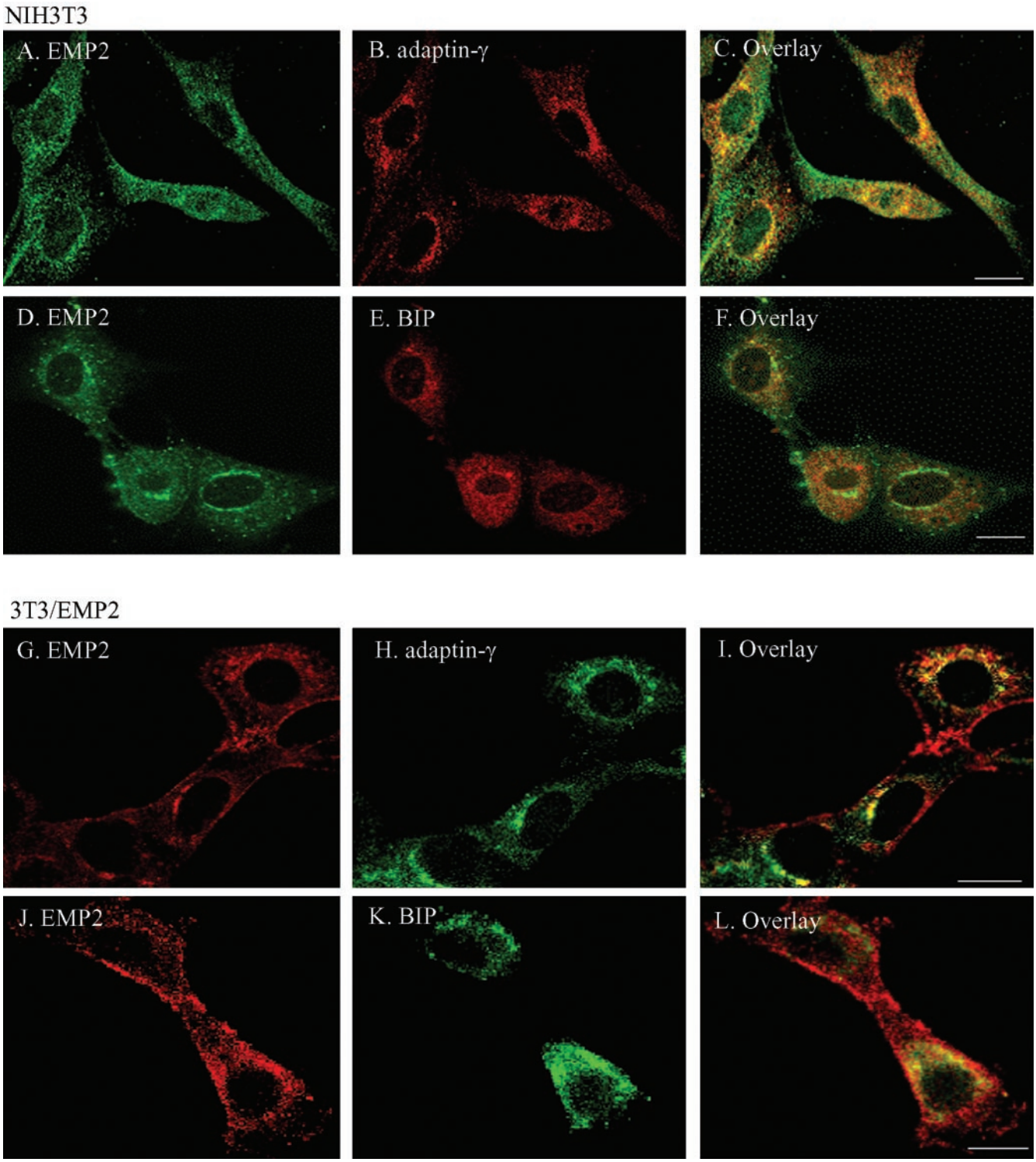

Figure 7. Perinuclear EMP2 is primarily localized in the Golgi apparatus. NIH3T3 cells (A–F) were fixed in 1.6% formaldehyde, permeabilized with 0.1% Triton X-100, and stained with antibodies to EMP2 (FITC; A and D), the Golgi protein γ-adaptin (Texas-Red, B), and the ER-chaperone protein BIP (Texas-Red, E). Single plane overlays are shown (C and F). 3T3/EMP2 cells (G–L) were fixed in 1.6% formaldehyde, permeabilized with 0.1% Triton X-100 and stained with antibodies to EMP2 (Texas-Red; G and J), γ-adaptin (FITC; H), and BIP (FITC; K). A single plane overlay is shown (I and L). Experiments were performed independently at least three times with similar results. Magnification, 600×. Bar, 15 μM.

ization between EMP2 and γ-adaptin may reflect the predominant residence of EMP2 in the Golgi apparatus and in a distinct endocytic itinerary shared by the GPI-AP pool. This distinct itinerary may involve recycling/trafficking microdomains that could account for the prominent localization of EMP2 in cytoplasmic compartments.

Mechanistically, it is intriguing to speculate how EMP2 alters caveolins and GPI-APs. EMP2 and caveolin-1 do not colocalize. EMP2 overexpression results in 3:1 EMP2:caveolin stoichiometric change and reduces steady-state levels of both caveolin-1 mRNA and protein. Thus, EMP2 does not seem to directly influence caveolin through biochemical interaction, but indirectly through suppression of caveolin-1 expression. We note that changes in caveolin-2 may be secondary to caveolin-1, because caveolin-1 expression stabilizes the caveolin-2 protein and allows its transport from the Golgi complex to the plasma membrane (Parolini *et al*., 1999).

Because there is a threefold greater reduction in caveolin-1 protein compared with mRNA, EMP2 seems to act on caveolin-1 expression at both the mRNA and protein level. The specific mechanism by which EMP2 influences caveolin-1 mRNA expression is unclear. At the protein level, we speculate that EMP2 and caveolin-bearing vesicles may compete for a shared, limiting machinery for their plasma membrane delivery. Failure to successfully compete may result in alternate destinations leading to accelerated degradation.

The control of GPI-APs by EMP2 is distinct from that of the caveolins. EMP2 does not significantly affect total GPI-APs levels within the cell, but rather it alters their localization. We speculate that this change is a direct result of EMP2, reflecting its role in the formation and efficient trafficking of caveolin-independent endosomes, some of which contain GPI-APs. On the other hand, it is possible that the change in GPI-APs is an indirect effect caused by caveolins or some yet unidentified mediating protein.

Abrami *et al*., 2001 recently proposed that a cross talk exists between caveolae and GPI-rich raft domains. This insight is functionally important because these alternate lipid raft microdomains bear distinct protein components and accordingly enable different patterns of recognition and signaling responsiveness. For example, different heterotrimeric G proteins partition to lipid raft or caveolae domains (Oh and Schnitzer, 2001). Analogously, EMP2 expression alters the levels of distinct integrins at the cell surface (e.g., augmenting $\alpha 6\beta 1$ while down-regulating $\alpha 5\beta 1$ integrins) (Wadehra *et al*., 2002). The present study extends this hypothesis, by showing that EMP2 itself can be a regulator of this caveolae-lipid raft cross talk. Accordingly, the relative levels of EMP2 and caveolin-1 may provide a mechanism to modulate patterns of receptor expression and the accompanying pattern of cellular responsiveness. The distinct composition of caveolae and GPI-AP lipid rafts suggests the corollary that EMP2 and caveolin-1 escort or segregate different proteins. The role of EMP2 in the cross talk of caveolae and GPI-AP lipid rafts thus suggests several testable predictions to better understand the formation of receptor signaling complexes at the cell surface.

ACKNOWLEDGMENTS

We thank Dr. T. Buckley (University of Victoria) for gifts of reagents. We are grateful to Drs. Lynn Gordon and A.K. Rajasekaran for critical reading of the manuscript. This work was supported by the Lymphoma Research Foundation of America, the Jonsson Comprehensive Cancer Center, the Granet-Mantle Cell Lymphoma Fund, the Ruzic Foundation, and the John Lloyd Foundation. M.W. is supported by a National Institutes of Health Tumor Immunology Training Grant fellowship (NIH 5-T32-CA009120-27).

REFERENCES

Abrami, L., Fivaz, M., Kobayashi, T., Kinoshita, T., Parton, R.G., and van der Goot, F.G. (2001). Cross-talk between caveolae and glycosylphosphatidylinositol-rich domains. J. Biol. Chem. *276*, 30729–30736.

Barry, R., Moore, S., Alonso, A., Ausio, J., and Buckley, J.T. (2001). The channel-forming protein proaerolysin remains a dimer at low concentrations in solution. J. Biol. Chem *276*, 551–554.

Ben Porath, I., Benvenisty, N. (1996). Characterization of a tumor-associated gene, a member of a novel family of genes encoding membrane glycoproteins. Gene. *183*, 69–75.

Ben Porath, I., Yanuka, O., Benvenisty, N. (1999). The tmp gene, encoding a membrane protein, is a c-Myc target with a tumorigenic activity. Mol. Cell Biol. *19*, 3529–3539.

Berditchevski, F. (2001). Complexes of tetraspanins with integrins: more than meets the eye. J. Cell Sci. *114*, 4143–4151.

Berditchevski, F., and Odintsova, E. (1999). Characterization of integrin-tetraspanin adhesion complexes: role of tetraspanins in integrin signaling. J. Cell Biol. *146*, 477–492.

Berger, P., Young, P., and Suter, U. (2002). Molecular cell biology of Charcot-Marie-Tooth disease. Neurogenetics *4*, 1–15.

Brancolini, C., Edomi, P., Marzinotto, S., and Schneider, C. (2000). Exposure at the cell surface is required for gas3/PMP22 To regulate both cell death and cell spreading: implication for the Charcot-Marie-Tooth type 1A and Dejerine-Sottas diseases. Mol. Biol. Cell *11*, 2901–2914.

Brown, D.A., and London, E. (1997). Structure of detergent-resistant membrane domains: does phase separation occur in biological membranes? Biochem. Biophys. Res. Commun. *240*, 1–7.

Brown, D.A., and London, E. (1998a). Functions of lipid rafts in biological membranes. Annu. Rev. Cell Dev. Biol. *14*, 111–136.

Brown, D.A., and London, E. (1998b). Structure and origin of ordered lipid domains in biological membranes. J. Membr. Biol. *164*, 103–114.

Brown, D.A., and London, E. (2000). Structure and function of sphingolipid- and cholesterol-rich membrane rafts. J. Biol. Chem. *275*, 17221–17224.

Chatterjee, S., Smith, E.R., Hanada, K., Stevens, V.L., and Mayor, S. (2001). GPI anchoring leads to sphingolipid-dependent retention of endocytosed proteins in the recycling endosomal compartment. EMBO J. *20*, 1583–1592.

Claas, C., Stipp, C.S., and Hemler, M.E. (2001). Evaluation of prototype transmembrane 4 superfamily protein complexes and their relation to lipid rafts. J. Biol. Chem. *276*, 7974–7984.

Daro, E., van der, S.P., Galli, T., and Mellman, I. (1996). Rab4 and cellubrevin define different early endosome populations on the pathway of transferrin receptor recycling. Proc. Natl. Acad. Sci. USA *93*, 9559–9564.

Diep, D.B., Nelson, K.L., Raja, S.M., Pleshak, E.N., and Buckley, J.T. (1998). Glycosylphosphatidylinositol anchors of membrane glycoproteins are binding determinants for the channel-forming toxin aerolysin. J. Biol. Chem *273*, 2355–2360.

Evans, W.H., and Martin, P.E. (2002). Gap junctions: structure and function (review). Mol. Membr. Biol. *19*, 121–136.

Fielding, P.E., and Fielding, C.J. (1996). Intracellular transport of low density lipoprotein derived free cholesterol begins at clathrin-coated pits and terminates at cell surface caveolae. Biochemistry *35*, 14932–14938.

Fivaz, M., Abrami, L., Tsitrin, Y., and van der Goot, F.G. (2001). Aerolysin from *Aeromonas hydrophila* and related toxins. Curr. Top. Microbiol. Immunol. *257*, 35–52.

Fra, A.M., Williamson, E., Simons, K., and Parton, R.G. (1995). De novo formation of caveolae in lymphocytes by expression of VIP21-caveolin. Proc. Natl. Acad. Sci. USA *92*, 8655–8659.

Galbiati, F., Razani, B., and Lisanti, M.P. (2001a). Emerging themes in lipid rafts and caveolae. Cell *106*, 403–411.

Galbiati, F., Volonte', D., Liu, J., Capozza, F., Frank, P.G., Zhu, L., Pestell, R.G., and Lisanti, M.P. (2001b). Caveolin-1 expression negatively regulates cell cycle progression by inducing G(0)/G(1) arrest via a p53/p21(WAF1/Cip1)-dependent mechanism. Mol. Biol. Cell *12*, 2229–2244.

Gargalovic, P., and Dory, L. (2001). Caveolin-1 and caveolin-2 expression in mouse macrophages. High density lipoprotein 3-stimulated secretion and a lack of significant subcellular co-localization. J. Biol. Chem. *276*, 26164–26170.

Gruenberg, J., and Maxfield, F.R. (1995). Membrane transport in the endocytic pathway. Curr. Opin. Cell Biol. *7*, 552–563.

Harder, T., Scheiffele, P., Verkade, P., and Simons, K. (1998). Lipid domain structure of the plasma membrane revealed by patching of membrane components. J. Cell Biol. *141*, 929–942.

Hasse, B., Bosse, F., and Muller, H.W. (2002). Proteins of peripheral myelin are associated with glycosphingolipid/cholesterol-enriched membranes. J. Neurosci. Res. *69*, 227–232.

Hemler, M.E. (2001). Specific tetraspanin functions. J. Cell Biol. *155*, 1103–1107.

Kobayashi, T., Vischer, U.M., Rosnoblet, C., Lebrand, C., Lindsay, M., Parton, R.G., Kruithof, E.K., and Gruenberg, J. (2000). The tetraspanin CD63/lamp3

cycles between endocytic and secretory compartments in human endothelial cells. Mol. Biol. Cell *11*, 1829–1843.

Kogo, H., and Fujimoto, T. (2000). Caveolin-1 isoforms are encoded by distinct mRNAs. Identification Of mouse caveolin-1 mRNA variants caused by alternative transcription initiation and splicing. FEBS Lett. *465*, 119–123.

Lang, D.M., Lommel, S., Jung, M., Ankerhold, R., Petrausch, B., Laessing, U., Wiechers, M.F., Plattner, H., and Stuermer, C.A. (1998). Identification of reggie-1 and reggie-2 as plasma membrane-associated proteins which cocluster with activated GPI-anchored cell adhesion molecules in non-caveolar micropatches in neurons. J. Neurobiol. *37*, 502–523.

Leitinger, B., and Hogg, N. (2002). The involvement of lipid rafts in the regulation of integrin function. J. Cell Sci. *115*, 963–972.

Levy, S., Todd, S.C., and Maecker, H.T. (1998). CD81 (TAPA-1): a molecule involved in signal transduction and cell adhesion in the immune system. Annu. Rev. Immunol. *16*, 89–109.

Lipardi, C., Nitsch, L., and Zurzolo, C. (2000). Detergent-insoluble GPI-anchored proteins are apically sorted in Fischer rat thyroid cells, but interference with cholesterol or sphingolipids differentially affects detergent insolubility and apical sorting. Mol. Biol. Cell *11*, 531–542.

Lusa, S., Blom, T.S., Eskelinen, E.L., Kuismanen, E., Mansson, J.E., Simons, K., and Ikonen, E. (2001). Depletion of rafts in late endocytic membranes is controlled by NPC1-dependent recycling of cholesterol to the plasma membrane. J. Cell Sci. *114*, 1893–1900.

Maecker, H.T., Todd, S.C., and Levy, S. (1997). The tetraspanin superfamily: molecular facilitators. FASEB J. *11*, 428–442.

Mayor, S. (1999). Analysis of the cell-surface distribution of GPI-anchored proteins. Methods Mol. Biol. *116*, 23–36.

Mayor, S., Sabharanjak, S., and Maxfield, F.R. (1998). Cholesterol-dependent retention of GPI-anchored proteins in endosomes. EMBO J. *17*, 4626–4638.

Melkonian, K.A., Ostermeyer, A.G., Chen, J.Z., Roth, M.G., and Brown, D.A. (1999). Role of lipid modifications in targeting proteins to detergent-resistant membrane rafts. Many raft proteins are acylated, while few are prenylated. J. Biol. Chem. *274*, 3910–3917.

Moffett, S., Brown, D.A., and Linder, M.E. (2000). Lipid-dependent targeting of G proteins into rafts. J. Biol. Chem. *275*, 2191–2198.

Moran, M., and Miceli, M.C. (1998). Engagement of GPI-linked CD48 contributes to TCR signals and cytoskeletal reorganization: a role for lipid rafts in T cell activation. Immunity *9*, 787–796.

Mukherjee, S., Ghosh, R.N., and Maxfield, F.R. (1997). Endocytosis. Physiol. Rev. *77*, 759–803.

Nelson, K.L., Brodsky, R.A., and Buckley, J.T. (1999). Channels formed by subnanomolar concentrations of the toxin aerolysin trigger apoptosis of T lymphomas. Cell Microbiol. *1*, 69–74.

Nichols, B.J. (2002). A distinct class of endosome mediates clathrin-independent endocytosis to the Golgi complex. Nat. Cell Biol. *4*, 374–378.

Nichols, B.J., Kenworthy, A.K., Polishchuk, R.S., Lodge, R., Roberts, T.H., Hirschberg, K., Phair, R.D., and Lippincott-Schwartz, J. (2001). Rapid cycling of lipid raft markers between the cell surface and Golgi complex. J. Cell Biol. *153*, 529–541.

Notterpek, L., Ryan, M.C., Tobler, A.R., and Shooter, E.M. (1999). PMP22 accumulation in aggresomes: implications for CMT1A pathology. Neurobiol. Dis. *6*, 450–460.

Oh, P., and Schnitzer, J.E. (2001). Segregation of heterotrimeric G proteins in cell surface microdomains. G(q) binds caveolin to concentrate in caveolae, whereas G(i) and G(s) target lipid rafts by default. Mol. Biol. Cell *12*, 685–698.

Ostermeyer, A.G., Paci, J.M., Zeng, Y., Lublin, D.M., Munro, S., and Brown, D.A. (2001). Accumulation of caveolin in the endoplasmic reticulum redirects the protein to lipid storage droplets. J. Cell Biol. *152*, 1071–1078.

Parker, M.W., van der Goot, F.G., and Buckley, J.T. (1996). Aerolysin – the ins and outs of a model channel-forming toxin. Mol. Microbiol. *19*, 205–212.

Parolini, I., *et al*. (1999). Expression of caveolin-1 is required for the transport of caveolin-2 to the plasma membrane. Retention of caveolin-2 at the level of the Golgi complex. J. Biol. Chem. *274*, 25718–25725.

Razani, B., *et al*. (2001). Caveolin-1 null mice are viable, but show evidence of hyper-proliferative and vascular abnormalities. J. Biol. Chem. *276*, 38121–38138.

Roberts, M., Barry, S., Woods, A., van der Sluijs, P., and Norman, J. (2001). PDGF-regulated rab4-dependent recycling of alphavbeta3 integrin from early endosomes is necessary for cell adhesion and spreading. Curr. Biol. *11*, 1392–1402.

Robinson, P.J. (1997). Signal transduction via GPI-anchored membrane proteins. Adv. Exp. Med. Biol. *419*, 365–370.

Rubinstein, E., Le Naour, F., Lagaudriere-Gesbert, C., Billard, M., Conjeaud, H., and Boucheix, C. (1996). CD9, CD63, CD81, and CD82 are components of a surface tetraspan network connected to HLA-DR and VLA integrins. Eur. J. Immunol. *26*, 2657–2665.

Sabharanjak, S., Sharma, P., Parton, R.G., and Mayor, S. (2002). GPI-anchored proteins are delivered to recycling endosomes via a distinct cdc42-regulated, clathrin-independent pinocytic pathway. Dev. Cell *2*, 411–423.

Sancho, S., Young, P., and Suter, U. (2001). Regulation of Schwann cell proliferation and apoptosis in PMP22-deficient mice and mouse models of Charcot-Marie-Tooth disease type 1A. Brain *124*, 2177–2187.

Schmidt, K., Schrader, M., Kern, H.F., and Kleene, R. (2001). Regulated apical secretion of zymogens in rat pancreas. Involvement of the glycosylphosphatidylinositol-anchored glycoprotein GP-2, the lectin ZG16p, and cholesterol-glycosphingolipid-enriched microdomains. J. Biol. Chem. 2001. *276*, 14315–14323.

Schnitzer, J.E., McIntosh, D.P., Dvorak, A.M., Liu, J., and Oh, P. (1995). Separation of caveolae from associated microdomains of GPI-anchored proteins. Science *269*, 1435–1439.

Schroeder, R.J., Ahmed, S.N., Zhu, Y., London, E., and Brown, D.A. (1998). Cholesterol and sphingolipid enhance the Triton X-100 insolubility of glycosylphosphatidylinositol-anchored proteins by promoting the formation of detergent-insoluble ordered membrane domains. J. Biol. Chem. *273*, 1150–1157.

Schubert, A.L., Schubert, W., Spray, D.C., and Lisanti, M.P. (2002). Connexin family members target to lipid raft domains and interact with caveolin-1. Biochemistry *41*, 5754–5764.

Sharma, D.K., Choudhury, A., Singh, R.D., Wheatley, C.L., Marks, D.L., and Pagano, R.E. (2003). Glycosphingolipids internalized via caveolar-related endocytosis rapidly merge with the clathrin pathway in early endosomes and form microdomains for recycling. J. Biol. Chem. *278*, 7564–7572.

Song, K.S., Scherer, P.E., Tang, Z., Okamoto, T., Li, S., Chafel, M., Chu, C., Kohtz, D.S., and Lisanti, M.P. (1996). Expression of caveolin-3 in skeletal, cardiac, and smooth muscle cells. Caveolin-3 is a component of the sarcolemma and co-fractionates with dystrophin and dystrophin-associated glycoproteins. J. Biol. Chem. *271*, 15160–15165.

Sotgia, F., *et al*. (2002). Intracellular retention of glycosylphosphatidyl inositol-linked proteins in caveolin-deficient cells. Mol. Cell Biol. *22*, 3905–3926.

Sternberg, P.W., and Schmid, S.L. (1999). Caveolin, cholesterol and Ras signalling. Nat. Cell Biol. *1*, E35–E37.

Stuermer, C.A., Lang, D.M., Kirsch, F., Wiechers, M., Deininger, S.O., and Plattner, H. (2001). Glycosylphosphatidyl inositol-anchored proteins and fyn kinase assemble in noncaveolar plasma membrane microdomains defined by reggie-1 and -2. Mol. Biol. Cell *12*, 3031–3045.

Taylor, V., and Suter, U. (1996). Epithelial membrane protein-2 and epithelial membrane protein-3, two novel members of the peripheral myelin protein 22 gene family. Gene. *175*, 115–120.

Tobler, A.R., Notterpek, L., Naef, R., Taylor, V., Suter, U., and Shooter, E.M. (1999). Transport of Trembler-J mutant peripheral myelin protein 22 is blocked in the intermediate compartment and affects the transport of the wild-type protein by direct interaction. J. Neurosci. *19*, 2027–2036.

Uittenbogaard, A., and Smart, E.J. (2000). Palmitoylation of caveolin-1 is required for cholesterol binding, chaperone complex formation, and rapid transport of cholesterol to caveolae. J. Biol. Chem. *275*, 25595–25599.

Uittenbogaard, A., Ying, Y., and Smart, E.J. (1998). Characterization of a cytosolic heat-shock protein-caveolin chaperone complex. Involvement in cholesterol trafficking. J. Biol. Chem. *273*, 6525–6532.

Wadehra, M., Iyer, R., Goodglick, L., and Braun, J. (2002). The tetraspan protein EMP2 interacts with beta 1 integrins and regulates adhesion. J. Biol. Chem. *277*, 41094–41100.

Wang, C.X., Wadehra, M., Fisk, B.C., Goodglick, L., and Braun, J. (2001). Epithelial membrane protein 2, a 4-transmembrane protein that suppresses B-cell lymphoma tumorigenicity. Blood *97*, 3890–3895.

Wary, K.K., Mariotti, A., Zurzolo, C., and Giancotti, F.G. (1998). A requirement for caveolin-1 and associated kinase Fyn in integrin signaling and anchorage-dependent cell growth. Cell *94*, 625–634.

Zuhorn, I.S., Kalicharan, R., and Hoekstra, D. (2002). Lipoplex-mediated transfection of mammalian cells occurs through the cholesterol-dependent clathrin-mediated pathway of endocytosis. J. Biol. Chem. *277*, 18021–18028.